# Data-Driven Model Development to Predict the Aging of a Li-ion Battery Pack in Electric Vehicles Representative Conditions

Rémy Mingant, Martin Petit, Sofiane Belaïd, Julien Bernard

# Data-driven model development to predict the aging of a Li-ion battery pack in electric vehicles representative conditions.

Rémy Mingant, Martin Petit, Sofiane Belaïd, Julien Bernard

HIGHLIGHTS

- A generic aging model of lithium-ion batteries has been developed and presented.
- This model is independent of the aging mechanism's knowledge.
- The calibration of the model is easy and fully automated.
- The model has been validated on several profiles including PHEV.

Keywords: Li-ion battery, Aging, State of Health, Generic Model, Easy training

An empirical generic Li-ion aging model, compatible with a large number of aging mechanisms without their a priori knowledge has been developed as well as a calibration methodology allowing its fast and automated parameter setting. This model has been applied to simulate the aging behavior of a 26 Ah cell. To train this model, a large aging test campaign has been conducted dedicated to both calibration and validation purposes. This one takes into account calendar, cycling, and their combinations. Based on the design of the aging campaign it is able to account for the effect of State Of Charge, temperature and current on aging. As its calibration is based on an automated process, it can be trained automatically and does not need expert knowledge for operation. Simulation data are validated to a 2% error in comparison to experimental data and is then validated for automotive applications.

# 1 Introduction

Nowadays, energy storage is a key technology area, with battery systems integrated into portable and security devices, in electric vehicles, and for green energy storage applications. Lithium-ion batteries are especially interesting because of their high energy and power density. Indeed, a Li-ion battery is one of the keys components of an electric vehicle. Its performance over time is sensitive to usage and environmental conditions, therefore remaining an obstacle to EV technology development [1]. This would eventually affect the price of a vehicle through the warranty expense for car manufacturers. Therefore, the development of tools to more accurately predict the degradation of Li-ion batteries during real-world use is critical. Over the last ten years, several partner organizations have been evaluating the aging of commercial Li-ion batteries through French research projects, i.e. - SIMSTOCK[2], SIMCAL [3], and MOBICUS [4].

The state of health (SoH) of a battery can be defined differently depending on the electrical behavior studied: battery state of energy and state of power. Hence, in our study, we will focus on the energy fading which is mainly proportional to battery capacity. SOH will be defined by the following equation:

$$SOH = \frac{Q_{act}}{Q_{nom}} \tag{1}$$

where $\mathrm{Q_{act}}$ is the actual capacity measured [Ah], and$\mathrm{Q_{nom}}$, the nominal capacity [Ah] of the battery.

With this definition, the SoH of a battery can be considered as a fuel tank which its volume is decreasing as a function of time, thermal and electric constraints [5–7].

Over their lifespan, batteries suffer from progressive degradation with reduced capacity, cycle life, and safety due to chemical changes to the electrodes. We can distinguish two types of aging: either from normal use (Cycle Aging) or just over time (Calendar Aging). The latter is known from the literature to depend on the battery state of charge (SoC) and temperature (T), whereas Cycling Aging depends on SOC, temperature, and current input [8].

Battery degradation mechanisms are complex phenomena and hard to fully comprehend. Analyses of these mechanisms are time-consuming and require large aging campaigns on a large number of cells. Furthermore, the constant evolution of battery chemistries doesn't simplify the task.

Laboratories determine SOH using a full charge and discharge cycle. This process is energy inefficient and difficult to apply in "online" applications because of the time needed to measure the capacity (>1h).

Thus, the aging of batteries remains a non-trivial field in which further research is needed in the areas of:

- Diagnostics: tools to rapidly diagnose the SOH of batteries,
- Modeling: models to predict the SOH of a battery depending on the application,
- Optimization: algorithms to optimize the SOH of a battery in use.

In this manner, battery SOH is a key indicator, since it can be used, firstly, to diagnose a battery in use: online tools implemented on battery management systems (BMS) can estimate the SOH of a Li-ion battery in use using temperature, current, and voltage sensors [9–12]. These tools use digital methods such as extended Kalman filtering or signal treatments in order to diagnose SOH. A comparison of different methodologies is presented in the review of Barai et al[13]. The majority of these diagnostic tools do not account for physical degradation mechanisms. Nonetheless, a certain number of studies have developed some methodology [14] based on differential analysis which can diagnose precisely the aging mechanism of a battery. As an example, Dubarry et al [15], use differential voltage which can estimate a loss of lithium inventory (LLI) and the loss of active material on the positive and negative electrodes at the lithiated or delithiated state. Such methods can be used for estimating the extent of Li-ion battery aging. Some other methods are based on entropy measurement [16] and also based on mechanical stress [17]. The latter are nevertheless laboratory technics and need costly equipment and more time than online tools, but results are more precise.

Secondly, for battery sizing: batteries aging models have been largely developed and can be separated into two main categories. On one hand, some physical models need high computational power and take into account electrochemical behavior such as electrolyte degradation, or active material loss. Simulation models have been developed [18–20] based on the growth of solid electrolyte interphase (SEI) that consumes the available lithium at the anode (positive/negative electrode). On the other hand, there are empirical models. These models are much diversified and need less computational power than physical models. Some rely on simple laws based on a power law and Arrhenius kinetics [21–23], mathematical functions, [24, 25], whereas others require electrical dynamics to predict the SoH [26]. For such models, an aging campaign on batteries is required to fit aging model parameters. These models are well suited for calendar aging as well as cycling aging for temperatures ranging between 20 and 60°C. For cycling aging at low temperatures, aging mechanisms such as Li plating on the anode [27–29] are known to take place. Some models account for theses mechanisms [4, 30–33]. Nonetheless, some aging mechanisms remain unknown and seeing that battery chemistries are continuously evolving, these mechanisms might remain elusive in the meantime. For almost all these models, calibration with battery aging campaign datasets is an issue due to the incomplete understanding of mechanisms, and the non-linearity of the models. In recent papers [34–36], data-driven aging models show good versatility independently of aging mechanism knowledge. This kind of model can also predict the minimal dataset needed to the training phase. Hence, the aging campaign could be dynamically reduced by removing operating conditions.

In light of these issues, this paper presents a new data-driven model that:

- is easy to calibrate (automatable): based on a set of representative data from an aging campaign,
- accurately predicts battery SoH even for complex aging profiles,
- self-adaptable to new mechanisms. For example, low-temperature aging mechanisms are automatically taken into account,
- computationally fast.

Our model has been implemented in a system simulation platform, Siemens PLM's software Simcenter Amesim$^{TM}$ [37] which integrates electro-thermal battery models. Such systems not only allow the use of complex simulators in predicting battery behavior in close-to-real-world conditions but can also be used to develop strategies to extend their lifespan [21].

# 2 Experimental

The studied battery was a prismatic PHEV-1 26 Ah with a Nickel Manganese Cobalt Oxide (NMC) cathode and a graphite anode. The characteristics of this battery are presented in Table 1.

*Table 1: Characteristics of the cells used in the study*

| | PHEV-1 |
|---|---|
| Mass [kg] | 0.7 |
| Chemistry | NMC/C |
| Tmin [°C] | -40 |
| Tmax [°C] | 60 |
| Capacity [Ah] | 26 |
| Min voltage [V] | 2.8 |
| Nominal voltage [V] | 3.7 |
| Max voltage [V] | 4.15 |
| Max charge current [A] | 50 |
| Max discharge current [A] | 98 |

Brand new batteries were used for the tests and stored at a medium state of charge (SoC) at low temperature (5°C). Before the characterization tests, the batteries were preconditioned with 5 charges and discharge cycles at C rate. For each aging condition, three cells were used to ensure the reproducibility of the results.

## 2.1 Test equipment

Aging tests [38] were performed on different test platforms within the MOBICUS consortium detailed in the acknowledgments. For electrical characterization tests, VMP3 potentiostats and bench tests type Digatron or ARBIN were used. During cycling tests, batteries were placed in climatic chambers to control their surrounding atmosphere and permit sufficient air convection to avoid self-heating effects.

Six types of tests were carried out in this study:

- A calendar test set was cells are placed on a climatic chamber at a defined SOC and temperature. This test aims to calibrate the initial model.
- A cycling test set was cells were placed on a climatic chamber and cycled to +/- 5% of their average SoC, in order to cycle in a SoC range of 10%, this aim of this test was also to calibrate a model.
- Calendar tests set were the initial SoC of the cell is set and the temperature of the climatic chamber varying to simulate seasons, and another one were the temperature is set and SOC varying between two states of charge. The purpose of these tests is to validate the model on calendar situation.
- A mixed cycling and calendar aging profile test.

- A PHEV aging test to validate the model with a combination of calendar and cycling aging.

Capacity fade and resistance growth were characterized by a check-up protocol described below.

## 2.2 Check-up protocols

Characterization tests were carried out every 6 weeks (5 weeks of aging, 1 week of characterization. This included:

- Capacity tests begin with a full charge at C/2 to the maximum cut-off voltage followed by a constant voltage charge to a current of C/20. Next, the cell is fully discharged at a constant current of C/10 to the minimum cut-off voltage. Finally, the cell is fully charged at a C/10 current to the maximum voltage, followed by a constant voltage phase to a current of C/20.
- The MOBICUS pulse characterization process, which can be summarized as follows: discharge (charge) 10s with 4C constant current, rest time for 2min, discharge (charge) 10% of the standard capacity of the battery with constant current, hold for 30 min, and repeat the process to discharge cut-off voltage (a maximum of 10 repetitions). Subsequently, the process is repeated on the charge.

## 2.3 Design of experiment

Figure 1 presents a summary of the aging process presented in this paper. Apart from PHEV test where 16 cells have been tested on a module, each test was carried out on 3 cells in order to ensure repeatability. Cells aged at rest state are represented in purple whereas cell aged under current loading are represented in blue. Calendar and cycling tests are used for model calibration, and present respectively:

- Calendar aging of cells on a shelf under a predefined SoC and temperature.
- Cycling test with predefined currents and SoC.

All the other aging tests were used to validate the model calibrated using calendar and aging tests.

The aim of thermal cycling and SOCV tests was to validate the behavior of the model in calendar conditions with respectively temperature and SoC which can vary as a function of the time, indeed, in the calendar calibration dataset, there is no variation of temperature and SoC.

In addition Calendar/Cycling and PHEV accelerating aging tests are used to validate the model with complex aging profiles melting calendar and cycling mechanisms. Hence, 72 % of cells are used to calibrate the model and 28 % for the validation.

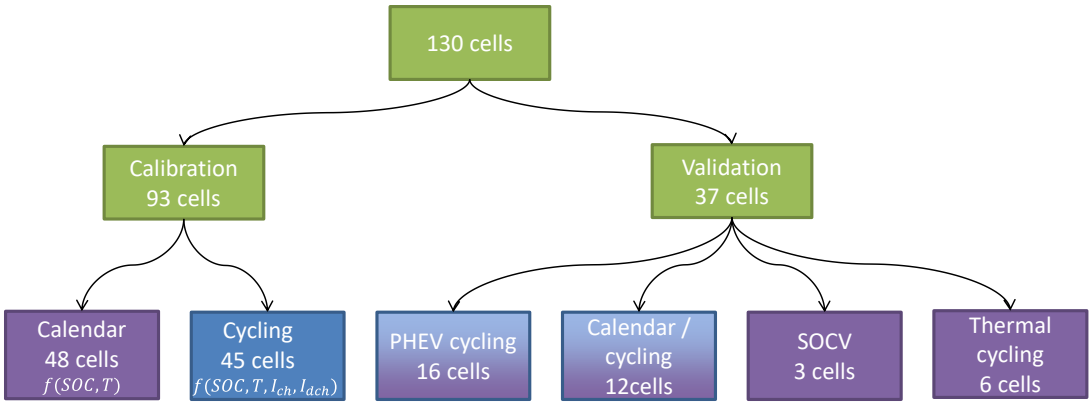


*Figure 1: diagram of tested cells on this study*

## Calibration tests

Simple calibration tests have been designed in order to represent most battery aging stress factors while being not to computationally expensive for long term simulation during parameter optimization. In these tests, aging stress factors are to be kept as constant as possible in order to decorrelate their effects.

### Calendar aging tests

The test matrix of conditions for calendar aging is presented in Table 2. This matrix is inspired by SIMCAL project [3] and uses a large range of temperature data (0 – 60°C) and SoC (0 – 100%) data for model calibration.

*Table 2: Test matrix of calendar aging*

| SoC [%]\T [°C] | 0 | 25 | 45 | 60 |
|---|---|---|---|---|
| 0 | | | X | |
| 30 | X | X | X | X |
| 65 | | X | X | X |
| 80 | X | X | X | X |
| 100 | X | X | X | X |

Battery conditions were electrically monitored once a month for 18 months. The SoC was then set at 25°C by a discharge at C after a full charge of the battery. Thereafter, batteries were placed in the climatic chamber at the corresponding aging temperature, without any electrical monitoring.

As illustrated in Figure 1 these results are to be used in order to calibrate the calendar part of the aging model.

### Cycling aging tests

The test matrix of conditions for cycling aging is presented in Table 3. This matrix is also inspired by the SIMSTOCK project and uses a large range of temperature data (0 – 45°C) and SoC (30 – 90%) data for model calibration. Cells were cycled to +/- 5% of their average SoC, in order to cycle in a SoC

range of 10%. As indicated in Table 3, the relative influence of the charge and discharge current ($I_C$ and $I_D$ respectively), to obtain a more complete matrix of data.

As illustrated in Figure 1 these results are used in the calibration of the cycling aging. Thanks to the plan of experiments, the model should be able to account for the temperature, SoC and charge and discharge rates (from 1/3C to 3C) impacts on aging.

*Table 3: Test matrix of cycling aging ($I_C$;$I_D$)*

| T (°C) | SOC (%) | $I_C$[C] | $I_D$[C] |
|---|---|---|---|
| 0 | 30 | 3 | 1 |
| | 80 | 3 | 3 |
| | 80 | 1 | 3 |
| | 90 | 1 | 1 |
| 25 | 30 | 1 | 3 |
| | 30 | 3 | 1 |
| | 65 | 1 | 1 |
| | 65 | 3 | 3 |
| | 80 | 3 | 1 |
| | 90 | 1 | 3 |
| 45 | 30 | 1 | 1 |
| | 30 | 3 | 3 |
| | 30 | 1/3 | 1/3 |
| | 65 | 3 | 3 |
| | 80 | 1 | 3 |

# Validation tests

### Thermal cycling aging tests

Thermal cycling aging tests were conducted to validate the calendar aging model with more realistic operating conditions (varying temperature). This aging test aimed to represent calendar aging during daily and seasonal variation as represented in Figure 2. Two thermal profiles were applied to the cells.

- The first one (cold season) consisted of one step at 0°C for 12h followed by another step at 30°C for 12h. This profile was repeated 80 times (80 days) followed by a check-up test
- The second one (hot season) was conducted with 30°C and 60°C steps. This profile was also repeated 80 times (80 days) followed by a check-up test.

These two seasons were looped 3 times to represent 3 years (accelerated).

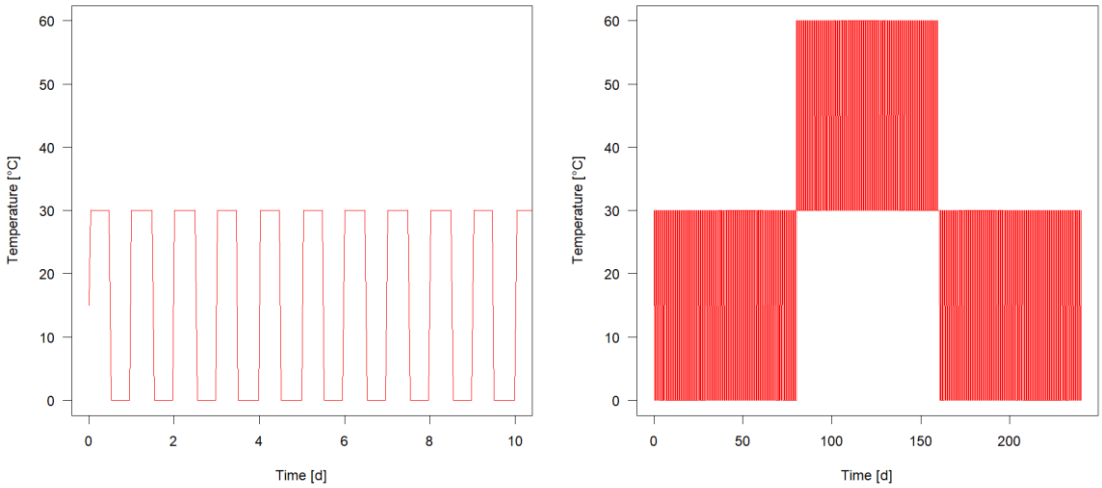


*Figure 2: Evolution of daily temperature on the cold season (left), and simplified seasonal variation of the temperature (right) for thermal cycling aging tests*

**State of Charge Variable (SoCV)**

Another campaign of calendar aging tests called SoCV , consisting of aging cells between 2 SoC values (80 and 30%) at 45°C was carried out. The protocol is detailed as:

- 11 weeks at 45°C and SoC= 30%
- 1 week check-up
- 5 weeks at 45°C and SoC= 80%
- 1 week check-up
- 5 weeks at 45°C and SoC= 80%
- 1 week check-up

These steps are repeated for the entire test duration. This test is used to validate the calendar aging of the cell and especially the fact that the variation of State of Charge of the cell does not prevent the good agreement between experiments and the model.

**Calendar/cycling tests**

A hybrid calendar/cycling aging test, which alternates the calendar and cycling phases, was carried out to simultaneously validate both the calendar and cycling model. These tests comprise a cycling period at 3C in charge and discharge, in a +/- 5% range of an average SoC, followed by normal calendar aging. To represent 2 cycles a day, the steps aggregate for one loop is a 12h. Test parameters are listed in Table 4.

The aim of this test is to check that calendar and cycling aging can be cumulated when they happen consecutively.

*Table 4: Operating conditions of Calendar/cycling tests (Ct= Cycling Time, total time=12h)*

| SoC [%]\T [°C] | 25 | 45 |
|---|---|---|
| 65 | Ct=2, 6h | Ct=2h |
| 80 | Ct=2, 6h | Ct=2h |

PHEV accelerating aging

A scenario with a daily use equivalent to 4 successive WLTC (Worldwide harmonized Light vehicles Test Procedures) was chosen. The power profile to be applied to the battery was obtained by a Simcenter Amesim PHEV vehicle simulator with the inputs of WLTC profiles. Then, this power profile was followed by a fast charge and a rest period of 4 hours. The complete cycle lasts 6 hours (Figure 3), with an acceleration factor of 4, i.e. 6 hours = 24 hours. The temperature profile in Figure 4 reproduces the temperature of the city of Nice in 2015. An offset of 5°C was also added to accelerate aging. This procedure was applied on a battery module with 16 cells in series.

This test aims at assessing the validity of the model in realistic conditions combining a realistic duty cycle and rest phases.

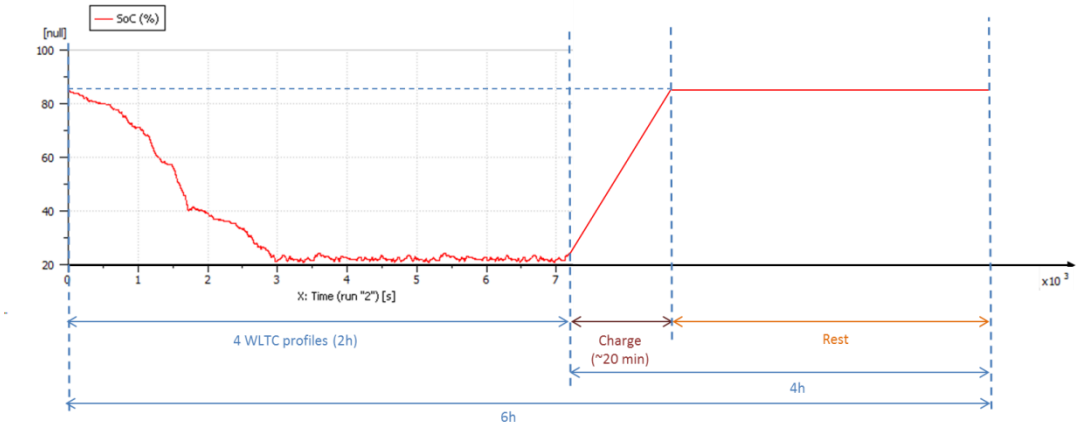


*Figure 3: Evolution of the battery SoC during a 6 hours cycle*

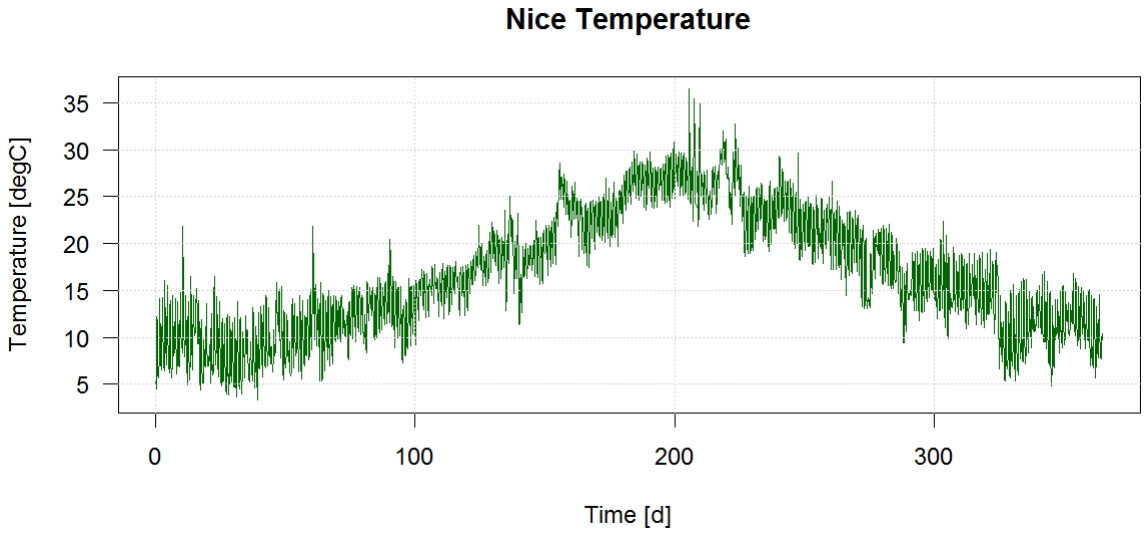


*Figure 4: Temperature of the city of Nice in 2015*

# 3 Model equations and calibration method

## 3.1 Model equations

The main objective of these comprehensive databases is the development of aging laws using an empirical approach. Laws and approaches depend on the partners and their research objectives [21].

Currently, the basic modeling approach of Simcenter Amesim has been described in [21]. In this approach, calendar aging depends on temperature and SoC, whereas cycling aging depends on temperature and cycling rate. Depending on the operating conditions and model parameters, the calendar aging capacity loss rate is applied when the cell is at rest or during discharge. The cycling aging capacity loss rate is used when the cell is in charge (I>0) at a sufficient rate. The equations of this model are presented eq (2) and (3):

$$\mathrm{k_{cal}} = \mathrm{B_{cal}} \exp\left(-\frac{\mathrm{Ea_{cal}}}{\mathrm{RT}}\right) \tag{2}$$

$$\frac{\mathrm{dQ_{loss}^{cal}}}{\mathrm{dt}} = \mathrm{z_{cal}}.k_{cal}.\left(\frac{\mathrm{Q_{loss}}}{\mathrm{k_{cal}}}\right)^{1-\frac{1}{\mathrm{z_{cal}}}}$$

$$\mathrm{k_{cyc}} = \mathrm{B_{cyc}} \exp\left(-\frac{\mathrm{Ea_{cyc}} + \alpha|\mathrm{I}|}{\mathrm{RT}}\right) \tag{3}$$

$$\frac{\mathrm{dQ_{loss}^{cyc}}}{\mathrm{dt}} = \frac{|\mathrm{I}|}{3600}.\mathrm{z_{cyc}}.\mathrm{k_{cyc}}.\left(\frac{\mathrm{Q_{loss}}}{\mathrm{k_{cyc}}}\right)^{1-\frac{1}{\mathrm{z_{cyc}}}}$$

Where $Q_{loss}^{cal}$ and $Q_{loss}^{cyc}$ are the loss capacity during the calendar phase and cycling phase respectively is the normalized capacity loss (%), $\mathrm{B_{cal}}$ and $\mathrm{B_{cyc}}$ are pre-exponential factors depending on SoC, $\mathrm{Ea_{cal}}$ and $\mathrm{Ea_{cyc}}$ are the activation energies (J.mol$^{-1}$), which evaluates the dependency of the calendar or cycling aging on temperature T(K), and $\mathrm{z_{cal}}$ and $\mathrm{z_{cyc}}$ are dimensionless constants for calendar and cycling aging respectively.

The temperature dependence for both calendar and cycling aging carried out through the application of the Arrhenius-rate laws, which predicts a faster capacity fade at high temperatures. Figure 6 shows that fast capacity fades are evident at high temperature under calendar aging, although the capacity fade is far higher at 0°C compared to 25 and 45°C. Such behavior is possibly related to cold-induced aging phenomena such as Li-plating that are not taken into account in the initial model.

As a consequence, the model from [21] has been generalized as a generic model (4):

$$\frac{dQ_{loss}^{gen}}{dt} = z_{gen}.B_{gen}.\left(\frac{Q_{loss}^{gen}}{B_{gen}}\right)^{(1-\frac{1}{z_{gen}})} \tag{4}$$

In this expression $\mathrm{B_{gen}}$ is a dimensionless pre-factor that depends on I, SoC and T, t is the aging time (s), and $\mathrm{z_{gen}}$ is a dimensionless constant.

The block diagram showing the calibration algorithm is presented in Figure 5. On this figure, one can observe that the first step is to be fit with calibration dataset on a linearized model using least-squares linear regressions in order to select a first set of relevant parameters. This first step aims to be computationally fast to select multiples parameters. Then the first set of parameters is then used in the generic model to be fitted with the same calibration data with a non-linear least squares regression. This model is slower than the previous one, but is more efficient to dissociate charge and discharges phases, and the use is closer to the aging tests on cells. Once the model fitted, the P-values calculated by the algorithm enable to identify one non-relevant parameter (value with the maximum P-value) which is removed. The fit and the statistic filtering steps are looped until max P-value is lower than 0.01. Finally, where all parameters are relevant, calibration parameters can be used on the generic model for the comparison with validation dataset.

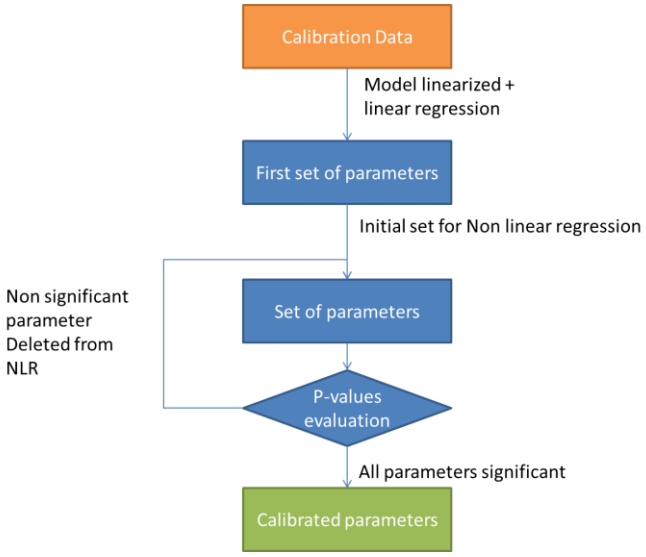


*Figure 5: Block diagram of calibration algorithm*

## 3.2 Aging model calibration

The identification of model parameters has been performed through R software facilities[39] on the calendar and cycling aging data. Aging conditions have been reproduced on a numerical model using the DeSolve R package and LSODA solver to evaluate $Q_{loss}^{gen}$ from eq 4. A non-linear regression algorithm (Levenberg-Marquardt) has been used to fit the parameters.

The resulting $B_{gen}$ and $z_{gen}$ are polynomial equations with:

$$\mathrm{B_{gen}} = B_1 + B_2.\mathrm{T}^2 + B_3.\mathrm{T} + B_4.I_{dch} + B_5.I_{ch} + B_6.\frac{1}{T^2} + B_7.\mathrm{T}.Ich + B_8.I_{ch}.SoC + B_9.I_{dch}.\frac{1}{T} + B_{10}.I_{dch}.T.SoC + B_{11}.I_{dch}.\frac{1}{T}.SoC \quad (5)$$

And

$$z_{gen0} = z_1 + z_2.T^2 + z_3.\frac{1}{T}.soc + z_4.\mathrm{I_{ch}} \quad (6)$$

Where $I_{ch}$ and$I_{dch}$are, respectively, the current value when I>0 and I<0 (default value is 0).

On the model, $z_{gen0}$ have been saturated between 0.5 and 1 by the mean of a hyperbolic tangent function:

$$z_{gen} = \frac{\tanh\left(2.\mathrm{z_{gen0}}\right)}{2} + 0.5 \quad (7)$$

The coefficients matrix of the estimated parameters is summarized in Table 5. This table lists the estimated coefficient and its standard error, t-value, a t-test associated with testing the significance of the "Estimate" column, Pr(>|t|), the p-value of the t-test (the proportion of the t distribution at that df which is greater than the absolute value of your t statistic). The asterisks following the Pr(>|t|) provide a visually accessible way of assessing whether the statistic met various criterions (*** for Pr(>|t|)<0.001, ** for Pr(>|t|)<0.01, … ). As we can see in the last column, all values are lower than 0.01 so each parameter is deemed useful to describe the model.

*Table 5: statistical study of fitted parameters on aging model training.*

| | Estimate | Std. Error | t value | Pr(>\|t\|) | |
|---|---|---|---|---|---|
| $\boldsymbol{B_1}$ | -5,63E-01 | 7,62E-02 | -7,39E+00 | 6,50E-13 | *** |
| $\boldsymbol{B_2}$ | -3,23E-06 | 4,37E-07 | -7,39E+00 | 6,70E-13 | *** |
| $\boldsymbol{B_3}$ | 2,54E-03 | 3,44E-04 | 7,39E+00 | 6,59E-13 | *** |
| $\boldsymbol{B_4}$ | 2,20E-03 | 4,09E-04 | 5,38E+00 | 1,16E-07 | *** |
| $\boldsymbol{B_5}$ | 8,03E-04 | 1,76E-04 | 4,57E+00 | 6,11E-06 | *** |
| $\boldsymbol{B_6}$ | 8,14E+03 | 1,10E+03 | 7,40E+00 | 6,32E-13 | *** |
| $\boldsymbol{B_7}$ | -2,70E-06 | 6,00E-07 | -4,50E+00 | 8,51E-06 | *** |
| $\boldsymbol{B_8}$ | -2,03E-07 | 7,67E-08 | -2,64E+00 | 8,48E-03 | ** |
| $\boldsymbol{B_9}$ | -6,83E-01 | 1,25E-01 | -5,48E+00 | 6,77E-08 | *** |
| $\boldsymbol{B_{10}}$ | -6,55E-08 | 9,30E-09 | -7,05E+00 | 6,50E-12 | *** |
| $\boldsymbol{B_{11}}$ | 6,02E-03 | 8,45E-04 | 7,13E+00 | 3,84E-12 | *** |
| $\boldsymbol{z_1}$ | 1,31E+00 | 5,28E-02 | 2,48E+01 | 5,93E-88 | *** |
| $\boldsymbol{z_2}$ | -1,12E-05 | 4,28E-07 | -2,63E+01 | 1,35E-94 | *** |
| $\boldsymbol{z_3}$ | 1,55E-01 | 1,00E-02 | 1,55E+01 | 5,85E-44 | *** |
| $\boldsymbol{z_4}$ | 1,31E-02 | 1,74E-03 | 7,54E+00 | 2,42E-13 | *** |

Once these parameters obtained equations 5 to 7 can be fed into equation 4 which is a text parameter from Simcenter Amesim battery model. The Figure 6 shows the results cycling aging for each temperature, in comparison with 3 models predictions. On this figure, cycling aging results are separated on 3 plots as a function of the room temperature. It can be seen that the largest lost capacity is shown in the plot at the lowest room temperature, and for the highest charge rates. This behavior can be explained by cold induced phenomena such as lithium plating aging mechanism. It can be noted that the 3C/3D condition seems to be less impacting than 3C/1D given the slope of the results. This is undoubtedly due to the cell temperature which is higher at high charging rate, and which improves the electrochemical kinetic properties, preventing the negative potential to drop below 0 V vs $Li^+/Li$ necessary for the li-plating mechanism.

Regarding 25 and 45 °C plots, the same behaviors are observed. The higher the current the higher the capacity loss is. Furthermore by comparing the cycling aging at 45 °C with the same 3C/3D condition, it appears that the SoC has an impact on aging since capacity loss is higher at 65 % SoC compared to 30 % SoC.

In Figure 6 the improvement brought about by the different steps can be seen:

- The first model presents the results from the first set of parameters with the linear model. The standard error of this model is 2.46 %, and some tests at low temperatures and high SoC presents larger errors than 8 %. In addition, at 45 °C all curves appear to be straighter than the other simulations which present fewer errors.
- The second model is fitted with the same parameters than the previous one but by means of the generic model. The standard error is 1.69 %, and as for the previous model, the test at 0°C and 90 % SoC shows a 7 % error. The other tests present better fit properties with fewer errors.
- The last model presents the best results with a standard error of 1.44 %, all calibration data are well fitted on this representation. This model is the one which is described following this paper.

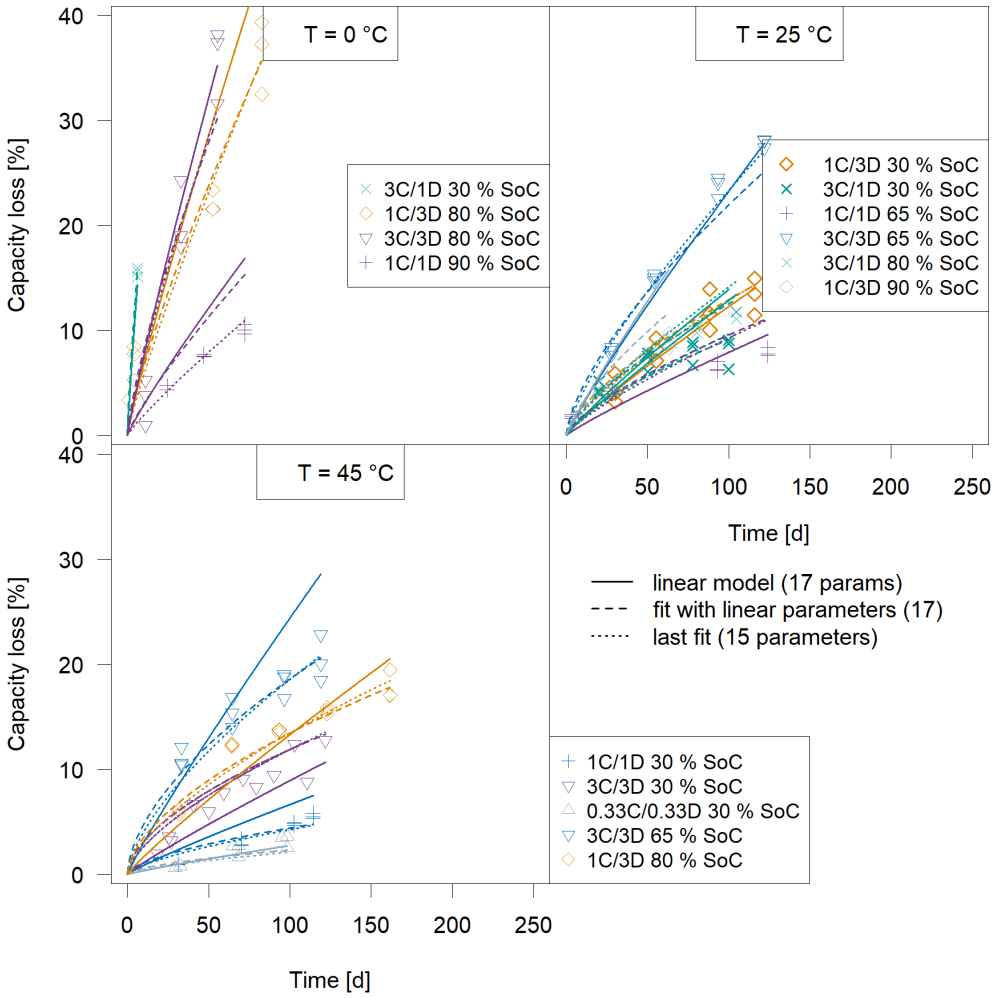


*Figure 6: Capacity loss plots for cycling aging tests with 3 fits levels of calibration process*

## Calibration comparison with reference model

### Calendar aging :

Figure 7 shows the battery capacity simulation vs. experimental results for calendar aging. In this figure, one can observe that the higher are the temperature and the SoC, the higher the capacity loss is. This behaviour is due to the degradation of the electrolyte whose kinetics will be all the greater the higher the cell temperature and voltage (thus the SoC). The calibration simulations from the reference model and the generic model are mostly in agreement with the experiments, except for the shapes of the aging curves at 60°C. This is probably due to the extreme aging conditions, where an irreversible aging mechanism predominates and is not accounted for during the beginning of the aging.

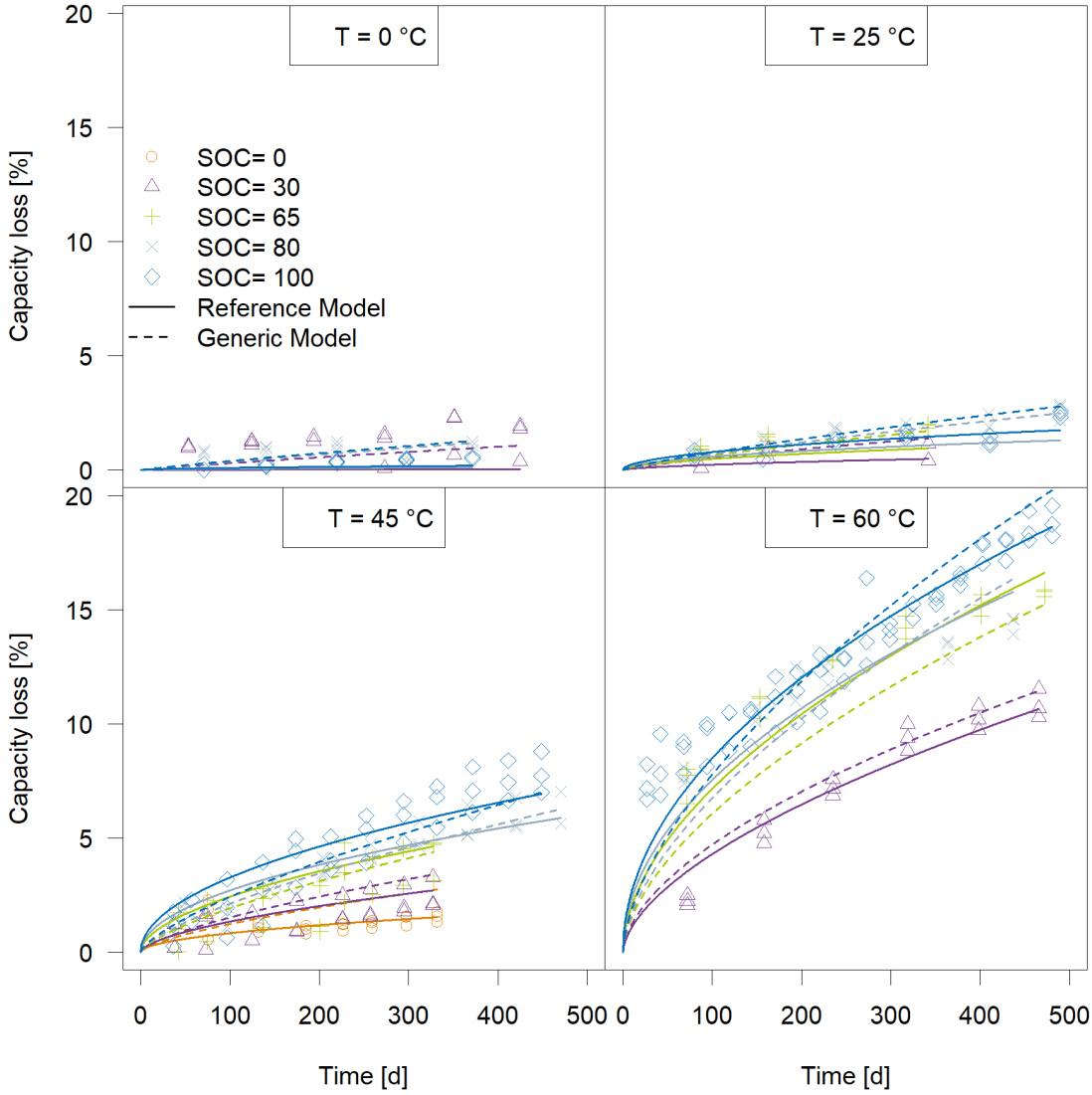


Figure 7: Simulations vs. experimental results for calendar aging.

**Cycling aging:**

For power cycling aging, the model results are presented in Figure 8. In this figure, one can observe differences between the reference and the generic model. Indeed, where test temperature is less than or equal to 25 °C, the reference model shows larges differences (up to 30 % capacity loss error) between experimental and simulation (low temperatures mechanisms are not taken into account in this model). This reference model is better at 45 °C with less than 5% capacity loss error. Generic model results show good accuracy for all temperatures with less than 3% capacity loss error.

Given the low accuracy of the reference model on calibration data, only generic model results are presented on the rest of the paper.

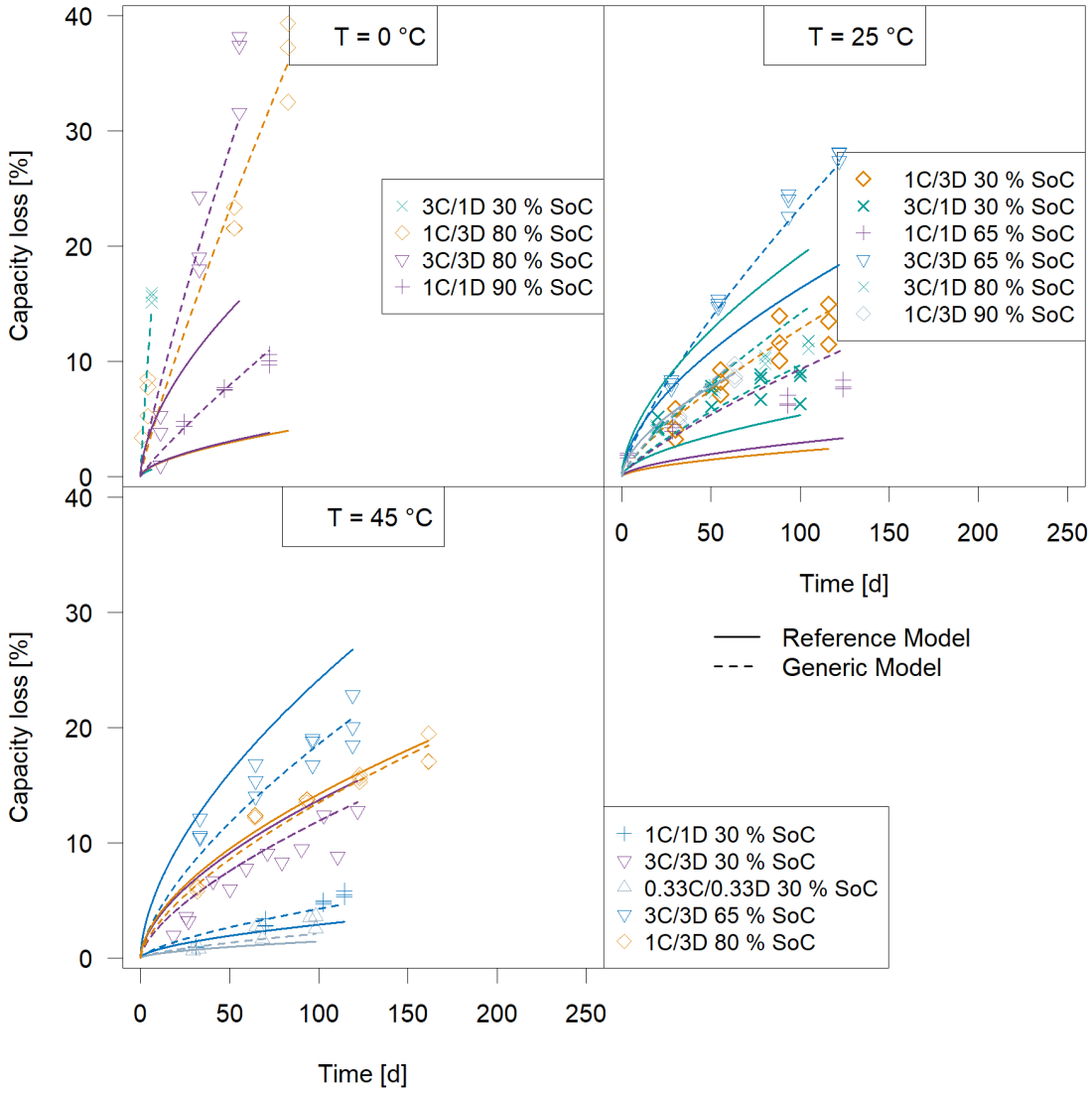


Figure 8: Simulation vs. experimental results for cycling aging

# 4 Results and Discussion

This section presents a comparison between simulation results and experimental data from the validation data set which have not been used for the model calibration step. The simulation results presented were obtained using an Amesim model and temperatures and current profiles (including for SoC setting) were applied exactly as cells tests. This part aims to validate the model and investigate the limits of its application.

Figure 9 shows the battery capacity simulation vs. experimental results for calendar aging with a SoC variation. As expected, the capacity loss is more significant at high SoC in calendar aging. However, the experimental data show regeneration of the capacity at 30% of SoC. This phenomenon is not considered by the model (monotonous equation) which explains the gap between experimental data and simulation data at this value of SoC. Regardless, the capacity loss is well predicted by the model in general.

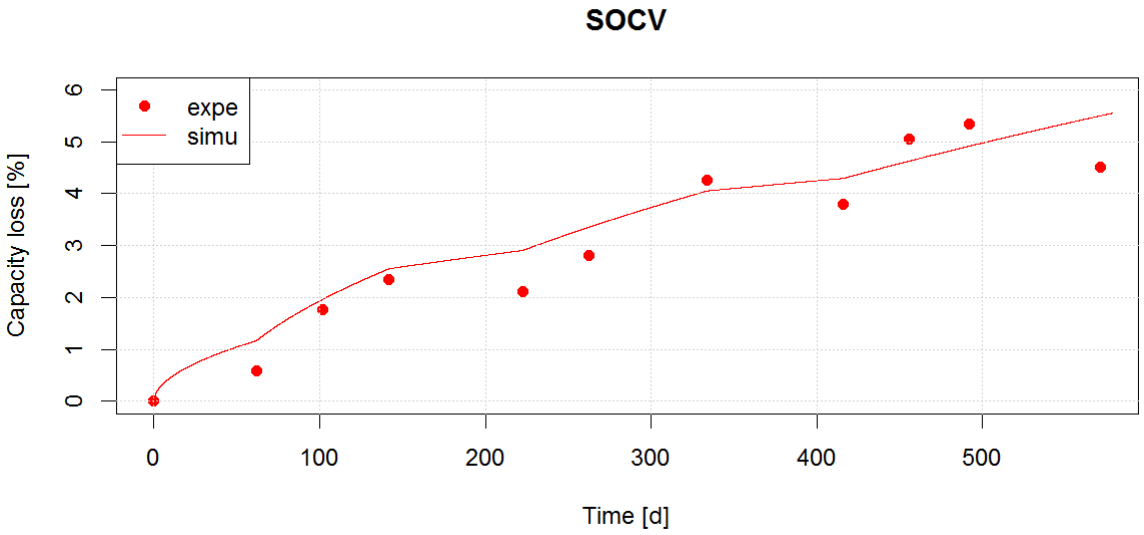


Figure 9: Simulation vs. experimental results for calendar aging with a SoC variation

Figure 10 shows the battery capacity simulation results vs. experimental results for calendar aging with a temperature variation at 65 and 100% SoC. In these simulation, the temperature profiles as a function of time were directly fed as inputs of the Simcenter Amesim battery model. The experimental data show a capacity increase (regeneration) when the temperature is cycled between 0°C and 30°C, especially at 100% of SoC. The model does not take this phenomenon into account, which explains the gap between experimental data and simulation data. At 65% of SoC, the regeneration is not significant, and so the model fits well with experimental results.

Figure 11 shows the battery capacity simulation results for the mix of calendar and cycling aging tests at 65% and 80% of SoC. In these simulations, a simple lumped thermal model has been used in order to predict the cell temperature which can vary under current solicitations. Using the signal library of Simcenter Amesim, current cycling and rest phases of the experiment were reproduced in the model.

The capacity loss is better predicted by the model when cycling time is 2h. for other cycling times, the model overestimates the capacity loss. This could be explained by a difference between the simulator and the experimental protocol. The model is validated for calendar and cycling aging.

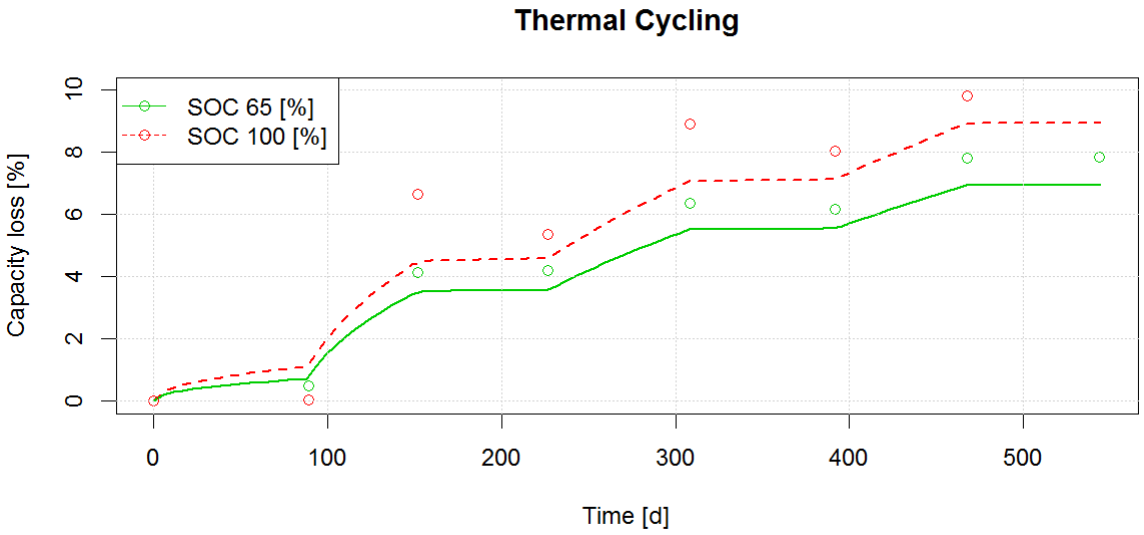


Figure 10: Simulation vs. experimental results for calendar aging with a temperature variation

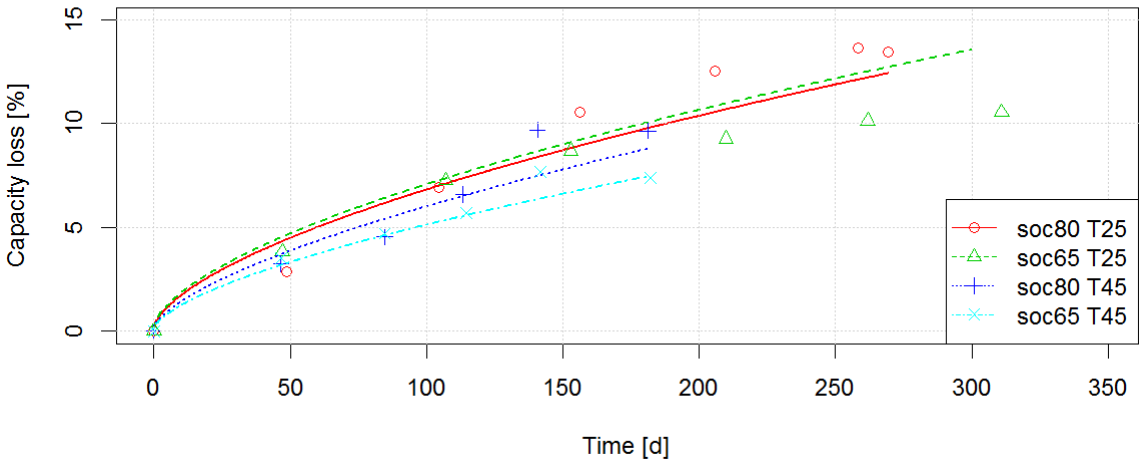


Figure 11: Simulation vs. experimental results for calendar/cycling aging with a SoC variation

Figure 12 shows PHEV accelerated aging results after 6 months of cycling, corresponding to a usage scenario of 2 years. On this plot, the time axis includes PHEV cycling and also check-up and rest time. The battery capacity decreased by 8%, and its internal resistance remained stable. To validate the aging model, the reference test was simulated completely taking into account all the rest and check-

ups. Cell temperature was simulated based on a lumped approach where the external temperature was the temperature setpoint of the climatic chamber as a function of time. Cell thermal parameters such as heat tranfer coefficient, thermal capacity were fitted against experimental data so that cell model temperature fits the experiment temperature throughout the experiment. PHEV cycling has been performed by using elements from Simcenter Amesim signal library and rest phase have also been added in order to account for periods of time when the test was stopped and also check-ups phases. In Figure 12, capacity losses estimated by our model (for a cell located at the center of the module) and measured battery are compared. The model gives a good estimation of the capacity losses, even in the case of a complex test involving dynamic cycling phases, continuous charge, calendar phases, and a strong variation of the outside temperature (seasonal cycles).

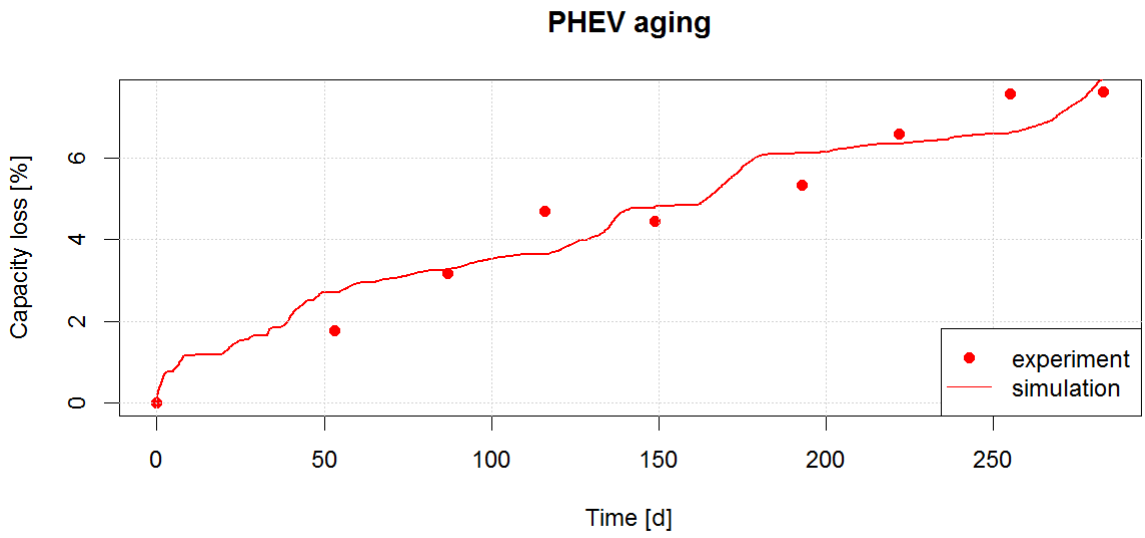


*Figure 12: Capacity loss of the 8th cell - measurement vs. simulation*

Hence, the generic model is more accurate than the reference one because it can adapt different aging mechanisms without preliminary be implemented by physicians.

A validation test has been done on several profiles and showcases good accuracy even with PHEV profile. Indeed, on other studies [34–36], validation is only done on simple constant charge and discharge profiles which are similar to the training dataset.

So as to train the generic model, it is however necessary to provide a large training dataset showing the largest operating conditions possible. Where operating conditions are too different from the training dataset, the model is not able to predict with accuracy the aging degradation of a battery.

In order to develop a model without conducting a specific aging campaign, training data could be provided by electric vehicles in operation via GSM communication.

# 5 Conclusions

The purpose of this study was to calibrate and test a data-driven battery aging model for an NMC/C Li-ion battery technology. The model approach is based on an empirical law depending on current, temperature, state of charge, and time. An algorithm was used to calibrate this model by R software using non-linear least square algorithm functions. The model appears to apply to a range of situations rather satisfactorily, including low-temperature aging, without prior mechanistic knowledge, which is not reflected in other state-of-the-art models. In a similar vein, a large range of battery chemistry aging can also be simulated using this approach.

Experimental data for calendar and cycling aging, and their combination, were validated by model simulation outputs. This kind of model could be extended to a large panel of empirical models when a time series model has to be described as a function of defined or measured parameters.

Such a model could be used to minimize the aging of a battery as a function of the application, for example by identifying the best management strategy with smart charges or smart cooling management.

The ease to calibrate this model makes it also possible to implement an auto adaptive model in a Battery Management System to diagnose battery state and forecast its second life application.

# Acknowledgements

Authors want to thank the 12 partners involved in the MOBICUS project: Renault (Leader); Siemens; Valeo; EDF; Controlsys; DBT; ERDF; CEA; IFP Energies nouvelles; IFSTTAR; EIGSI; IMS-Univ Bordeaux. Invited partners are: PSA; Saft; UTC; La Poste. This work obtained financial support from BPI France, the Conseil Général des Yvelines and the Conseil Régional du Nord-Pas de Calais.

Authors want also to thank Gaurav Joshi and David Beck for their careful rereading and constructive comments.

# References


1 Gandoman F.H., Jaguemont J., Goutam S., Gopalakrishnan R., Firouz Y., Kalogiannis T., Omar N., van Mierlo J. (2019) Concept of reliability and safety assessment of lithium-ion batteries in electric vehicles: Basics, progress, and challenges, *Applied Energy* **251**, 113343. DOI: 10.1016/j.apenergy.2019.113343.

2 Gyan P., Aubret P., Hafsaoui J., Sellier F., Bourlot S., Zinola S., Badin F. (2013) Experimental Assessment of Battery Cycle Life Within the SIMSTOCK Research Program, *Oil and Gas Science and Technology - Rev.IFP Energies nouvelles* **68**, 1, 137–147. DOI: 10.2516/ogst/2013106.

3 Grolleau S., Molina-Concha B., Delaille A., Revel R., Bernard J., Pelissier S., Peter J. (2013) The French SIMCAL Research Network For Modelling of Calendar Aging for Energy Storage System in EVs And HEVs - EIS Analysis on LFP/C Cells, *ECS Transactions* **45**, 13, 73–81. DOI: 10.1149/04513.0073ecst.

4 Belaid S., Mingant R., Petit M., Martin J., Bernard J. Strategies to Extend the Lifespan of Automotive Batteries through Battery Modeling and System Simulation: The MOBICUS Project, in *2017 IEEE Vehicle Power and Propulsion Conference (VPPC)*, pp. 1–9.

5 Bian X., Liu L., Yan J. (2019) A model for state-of-health estimation of lithium ion batteries based on charging profiles, *Energy* **177**, 57–65. DOI: 10.1016/j.energy.2019.04.070.

6 Berecibar M., Gandiaga I., Villarreal I., Omar N., van Mierlo J., van den Bossche P. (2016) Critical review of state of health estimation methods of Li-ion batteries for real applications, *Renewable and Sustainable Energy Reviews* **56**, 572–587. DOI: 10.1016/j.rser.2015.11.042.

7 Li Y., Abdel-Monem M., Gopalakrishnan R., Berecibar M., Nanini-Maury E., Omar N., van den Bossche P., van Mierlo J. (2018) A quick on-line state of health estimation method for Li-ion battery with incremental capacity curves processed by Gaussian filter, *J.Power Sources* **373**, 40–53. DOI: 10.1016/j.jpowsour.2017.10.092.

8 Redondo-Iglesias E., Venet P., Pelissier S. (2018) Calendar and cycling ageing combination of batteries in electric vehicles, *Microelectronics Reliability* **88-90**, 1212–1215. DOI: 10.1016/j.microrel.2018.06.113.

9 Mingant R., Bernard J., Sauvant-Moynot V. (2016) Novel state-of-health diagnostic method for Li-ion battery in service, *Applied Energy* **183**, 390–398. DOI: 10.1016/j.apenergy.2016.08.118.

10 Di Domenico D., Pognant-Gros P., Petit M., Creff Y. (2015) State of Health estimation for NCA-C Lithium-ion cells, in *2015 IFAC Workshop on Engine and Powertrain Control, Simulation and Modeling*, Sciarretta A., Paolino T. (eds.).

11 Goh T., Park M., Seo M., Kim J.G., Kim S.W. (2018) Successive-approximation algorithm for estimating capacity of Li-ion batteries, *Energy* **159**, 61–73. DOI: 10.1016/j.energy.2018.06.116.

12 Lucu M., Martinez-Laserna E., Gandiaga I., Camblong H. (2018) A critical review on self-adaptive Li-ion battery ageing models, *J.Power Sources* **401**, 85–101. DOI: 10.1016/j.jpowsour.2018.08.064.

13 Barai A., Uddin K., Dubarry M., Somerville L., McGordon A., Jennings P., Bloom I. (2019) A comparison of methodologies for the non-invasive characterisation of commercial Li-ion cells, *Progress in Energy and Combustion Science* **72**, 1–31. DOI: 10.1016/j.pecs.2019.01.001.

14 Li Y., Liu K., Foley A.M., Zülke A., Berecibar M., Nanini-Maury E., van Mierlo J., Hoster H.E. (2019) Data-driven health estimation and lifetime prediction of lithium-ion batteries: A review, *Renewable and Sustainable Energy Reviews* **113**, 109254. DOI: 10.1016/j.rser.2019.109254.

15 Dubarry M., Berecibar M., Devie A., Anseán D., Omar N., Villarreal I. (2017) State of health battery estimator enabling degradation diagnosis: Model and algorithm description, *Journal of Power Sources* **360**, 59–69. DOI: 10.1016/j.jpowsour.2017.05.121.

16 Maher K., Yazami R. (2014) A study of lithium ion batteries cycle aging by thermodynamics techniques, *J.Power Sources* **247**, 527–533. DOI: 10.1016/j.jpowsour.2013.08.053.

17 Cannarella J., Arnold C.B. (2014) State of health and charge measurements in lithium-ion batteries using mechanical stress, *J.Power Sources* **269**, 7–14. DOI: 10.1016/j.jpowsour.2014.07.003.

18 Prada E., Di Dominico D., Creff Y., Bernard J., Sauvant-Moynot V. (eds.) (2011) *A coupled 0D electrochemical ageing & electro-thermal Li-ion modeling approach for HEV/PHEV*, Chicago.

19 Liu Y., Xie K., Pan Y., Wang H., Li Y., Zheng C. (2018) Simplified modeling and parameter estimation to predict calendar life of Li-ion batteries, *Solid State Ionics* **320**, 126–131. DOI: 10.1016/j.ssi.2018.02.038.

20 Safari M., Morcrette M., Teyssot A., Delacourt C. (2009) Multimodal Physics-Based Aging Model for Life Prediction of Li-Ion Batteries, *J.Electrochem.Soc.* **156**, 3, A145-A153. DOI: 10.1149/1.3043429.

21 Petit M., Prada E., Sauvant-Moynot V. (2016) Development of an empirical aging model for Li-ion batteries and application to assess the impact of Vehicle-to-Grid strategies on battery lifetime, *Applied Energy* **172**, 398–407. DOI: 10.1016/j.apenergy.2016.03.119.

22 Wang J., Liu P., Hicks-Garner J., Sherman E., Soukiazian S., Verbrugge M., Tataria H., Musser J., Finamore P. (2011) Cycle-life model for graphite-LiFePO4 cells, *J.Power Sources* **196**, 8, 3942–3948. DOI: 10.1016/j.jpowsour.2010.11.134.

23 Bloom I., Cole B.W., Sohn J.J., Jones S.A., Polzin E.G., Battaglia V.S., Henriksen G.L., Motloch C., Richardson R., Unkelhaeuser T., Ingersoll D., Case H.L. (2001) An accelerated calendar and cycle life study of Li-ion cells, *J.Power Sources* **101**, 2, 238–247. DOI: 10.1016/S0378-7753(01)00783-2.

24 Ecker M., Gerschler J.B., Vogel J., Käbitz S., Hust F., Dechent P., Sauer D.U. (2012) Development of a lifetime prediction model for lithium-ion batteries based on extended accelerated aging test data, *J.Power Sources* **215**, 0, 248–257. DOI: 10.1016/j.jpowsour.2012.05.012.

25 Baghdadi I., Briat O., Delétage J.-Y., Gyan P., Vinassa J.-M. (2016) Lithium battery aging model based on Dakin's degradation approach, *J.Power Sources* **325**, 273–285. DOI: 10.1016/j.jpowsour.2016.06.036.

26 Baghdadi I., Briat O., Gyan P., Vinassa J.M. (2016) State of health assessment for lithium batteries based on voltage–time relaxation measure, *Electrochimica Acta* **194**, 461–472. DOI: 10.1016/j.electacta.2016.02.109.

27 Waldmann T., Hogg B.-I., Wohlfahrt-Mehrens M. (2018) Li plating as unwanted side reaction in commercial Li-ion cells – A review, *Journal of Power Sources* **384**, 107–124. DOI: 10.1016/j.jpowsour.2018.02.063.

28 Yang X.-G., Ge S., Liu T., Leng Y., Wang C.-Y. (2018) A look into the voltage plateau signal for detection and quantification of lithium plating in lithium-ion cells, *Journal of Power Sources* **395**, 251–261. DOI: 10.1016/j.jpowsour.2018.05.073.

29 Gao Y., Jiang J., Zhang C., Zhang W., Jiang Y. (2018) Aging mechanisms under different state-of-charge ranges and the multi-indicators system of state-of-health for lithium-ion battery with Li(NiMnCo)O2 cathode, *Journal of Power Sources* **400**, 641–651. DOI: 10.1016/j.jpowsour.2018.07.018.

30 Yang X.-G., Leng Y., Zhang G., Ge S., Wang C.-Y. (2017) Modeling of lithium plating induced aging of lithium-ion batteries: Transition from linear to nonlinear aging, *Journal of Power Sources* **360**, 28–40. DOI: 10.1016/j.jpowsour.2017.05.110.

31 Lin X., Hao X., Liu Z., Jia W. (2018) Health conscious fast charging of Li-ion batteries via a single particle model with aging mechanisms, *Journal of Power Sources* **400**, 305–316. DOI: 10.1016/j.jpowsour.2018.08.030.

32 Legrand N., Knosp B., Desprez P., Lapicque F., Raël S. (2014) Physical characterization of the charging process of a Li-ion battery and prediction of Li plating by electrochemical modeling, *J.Power Sources* **245**, 208–216.

33 Bai G., Wang P. (2016) An internal state variable mapping approach for Li-Plating diagnosis, *Journal of Power Sources* **323**, 115–124. DOI: 10.1016/j.jpowsour.2016.05.040.

34 Mathieu R., Baghdadi I., Briat O., Gyan P., Vinassa J.-M. (2017) D-optimal design of experiments applied to lithium battery for ageing model calibration, *Energy* **141**, 2108–2119. DOI: 10.1016/j.energy.2017.11.130.

35 Lucu M., Martinez-Laserna E., Gandiaga I., Liu K., Camblong H., Widanage W.D., Marco J. (2020) Data-driven nonparametric Li-ion battery ageing model aiming at learning from real operation data – Part A: Storage operation, *Journal of Energy Storage* **30**, 101409. DOI: 10.1016/j.est.2020.101409.

36 Lucu M., Martinez-Laserna E., Gandiaga I., Liu K., Camblong H., Widanage W.D., Marco J. (2020) Data-driven nonparametric Li-ion battery ageing model aiming at learning from real operation data - Part B: Cycling operation, *Journal of Energy Storage* **30**, 101410. DOI: 10.1016/j.est.2020.101410.

37 Siemens Digital Industry Software (2017) Simcenter Amesim. Available at: https:// www.plm.automation.siemens.com/global/fr/products/simcenter/simcenter-amesim.html.

38 Ben-Marzouk M., Chaumond A., Redondo-Iglesias E., Montaru M., Pélissier S. (2016) Experimental Protocols and First Results of Calendar and/or Cycling Aging Study of Lithium-Ion Batteries – the MOBICUS Project, *WEVJ* **8**, 2, 388–397. DOI: 10.3390/wevj8020388.

39 R Development Core Team *R: A Language and Environment for Statistical Computing*, R Foundation for Statistical Computing. ISBN: 3-900051-07-0.